Intermodal stimulated Brillouin scattering in two-mode fibers

Kwang Yong Song,[1,*] Yong Hyun Kim,[1] and Byoung Yoon Kim[2]

[1]*Department of Physics, Chung-Ang University, Seoul 156-756, South Korea*

[2]*Department of Physics, Korea Advanced Institute of Science and Technology, Daejeon 305-701, South Korea*

**Corresponding author: songky@cau.ac.kr*

Received February 28, 2013; revised April 20, 2013; accepted April 22, 2013;
posted April 24, 2013 (Doc. ID 186190); published May 20, 2013

Characterization of stimulated Brillouin scattering (SBS) in an elliptic-core two-mode fiber is experimentally demonstrated. The LP_{01} or LP_{11} mode is selectively launched to a fiber under test by a mode-selective coupler as a Brillouin pump, and the Brillouin gain spectra are analyzed for different mode pairs of the pump and probe waves. Intermodal SBS between counterpropagating LP_{01} and LP_{11} modes is observed, and the efficiency is measured to be about 58% of that of the SBS between the LP_{01} modes.

OCIS codes: (060.1810) Buffers, couplers, routers, switches, and multiplexers; (060.2310) Fiber optics; (290.5900) Scattering, stimulated Brillouin.

http://dx.doi.org/10.1364/OL.38.001805

Recently, mode division multiplexing with two- or few-mode fibers has attracted considerable attention as a new dimension for increasing the capacity of communication systems [1–3], where an elliptic-core (e-core) two-mode fiber (TMF) can provide the simplest platform by supporting only two optical modes (LP_{01} and LP_{11}) with stable orientation of the lobes in the LP_{11} mode [4]. So far, most of the studies on stimulated Brillouin scattering (SBS) in optical fibers have been performed based on single-mode fibers (SMFs), with a few exceptional cases of two- or few-mode fibers, such as the report on forward SBS between copropagating LP_{01} and LP_{11} modes based on TMFs [5], and more recently, the modeling of the intermodal SBS between LP_{01} and higher-order symmetric LP_{0n} modes based on higher-order mode fibers with large effective areas [6]. In this Letter, we present the characterization of the SBS between the same and different optical modes counterpropagating in a 100 m TMF. A mode-selective coupler (MSC) [7–9] is used to selectively launch the LP_{01} or the LP_{11} mode to the TMF as a Brillouin pump, and the Brillouin gain spectra (BGS) of counterpropagating probe waves are analyzed for different pairs of the pump–probe modes (LP_{01} – LP_{01}, LP_{11}–LP_{01}, LP_{01} – LP_{11}, LP_{11}–LP_{11}). Intermodal SBS is observed between the LP_{01} and the LP_{11} modes, and the efficiency is measured to be about 58% of that of the SBS between the LP_{01} modes. To the best of our knowledge, our result is the first report on the backward intermodal SBS between symmetric (LP_{01}) and antisymmetric (LP_{11}) optical modes.

An MSC is a directional coupler composed of a SMF and a TMF, in which the propagation constant of the LP_{01} mode of the SMF matches that of the LP_{11} mode of the TMF for mode coupling between them [7]. One can selectively launch the LP_{01} or the LP_{11} mode to the TMF as depicted in Fig. 1(a), or separate the signals of different modes of the TMF into different ports as shown in Fig. 1(b). The MSC used in our experiment was a polished-type one with a coupling efficiency (input, LP_{01} mode in the SMF; output, LP_{11} mode in the TMF) of about 80%, and a mode extinction ratio (LP_{11}/LP_{01}) in the coupled port of about 23 dB.

The experimental setup for measurement of the SBS in a TMF is shown in Fig. 2, where the structure of a fiber under test (FUT) is depicted in the inset. A 1550 nm DFB laser diode (LD) was used as a light source, and the output was divided by a 50/50 coupler into pump and probe arms. The probe wave was generated by a single-sideband modulator (SSBM) and a microwave synthesizer with the optical frequency downshifted from the carrier in the vicinity of the Brillouin frequency (ν_B) of the FUT (~10.64 GHz). The pump and the probe waves were amplified by Er-doped fiber amplifiers (EDFAs) with the output power controlled, and launched to an FUT from opposite ends. Polarization controllers (PCs) were used for the pump and probe waves to maximize the Brillouin gain for each measurement. The probe wave was detected by a 125 MHz photoreceiver through a variable optical attenuator (VOA).

The FUT was a 100 m *e*-core TMF with an index difference Δ of 0.6% and a core radius of 5.4 μm × 3.6 μm, which guides only the LP_{01} and the LP_{11} even modes with the LP_{11} odd mode cutoff at the operation wavelength [8]. The measured birefringence Δn of the fiber (for the LP_{01} mode) is about 3.5×10^{-5}. One end of the FUT was spliced to a lead fiber (SMF) of the probe arm with some transverse offset, so the input power ratio of the LP_{01} mode to the LP_{11} mode in the probe wave was about 50/50. Figure 3(a) shows the loss of the probe wave according to the bending radius of the TMF. The LP_{11}

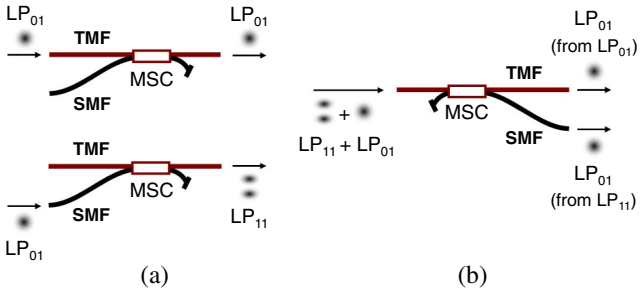

Fig. 1. Functions of the MSC: (a) selective launching of LP_{01} or LP_{11} mode to the TMF. (b) Separation of LP_{01} and LP_{11} of the TMF into different ports.

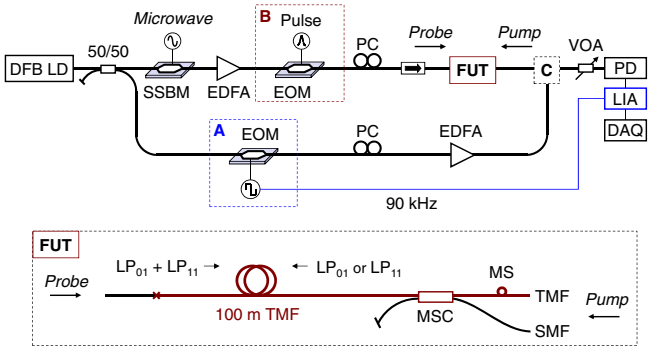

Fig. 2. Experimental setup: SSBM, single-sideband modulator; EOM, electro-optic modulator; EDFA, Er-doped fiber amplifier; VOA, variable optical attenuator; PC, polarization controller; LIA, lock-in amplifier; MS, mode stripper (by bending).

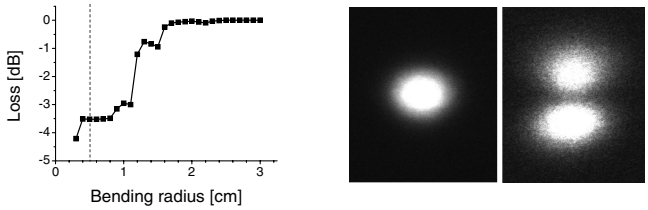

Fig. 3. (a) Loss of the probe wave as a function of the bending radius. Note the dashed line indicates the bending radius used for the mode strip of the LP_{11} mode. (b) Far-field patterns of the pump wave with the LP_{01} (left) or the LP_{11} (right) mode launched by the MSC.

mode could be removed (> 99%) at a bending radius of 0.5 cm (dashed line), which was used for a mode stripper (MS) in the measurement.

An MSC is located at the other end of the FUT for selective launching of the LP_{01} or the LP_{11} mode as the pump, and also for separating the LP_{01} and the LP_{11} modes of the probe wave into different ports. Figure 3(b) depicts far-field patterns of the pump wave with selective launching of the LP_{01} (left) and the LP_{11} (right) modes by the MSC. The connection (inset "C" in Fig. 2) between the MSC ports (SMF, TMF), the pump arm, and the detector was determined according to the target modes of the pump and probe waves, as listed in Table 1. Since the TMF port of the MSC is used for launching or detecting only the LP_{01} mode, an MS was inserted to remove the effect of the LP_{11} mode crosstalk (inset "FUT" in Fig. 2).

At first, the Brillouin gain spectrum (BGS) was measured by applying lock-in detection, where the pump wave was chopped with an electro-optic modulator (inset "A" in Fig. 2) and the probe signal was analyzed by a lock-in amplifier (LIA). The powers of the pump and the probe were 10 and 0 dBm, respectively, and the frequency offset between the pump and the probe was swept from 10.2 to 11.2 GHz.

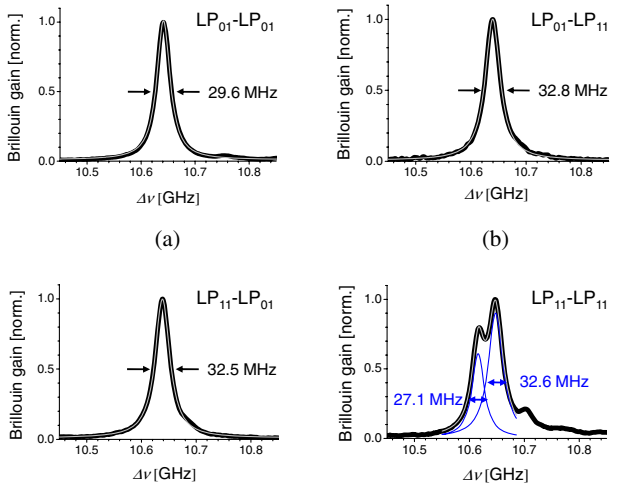

Fig. 4. Measured BGS for the pump–probe pair of (a) LP_{01} – LP_{01}, (b) LP_{01}–LP_{11}, (c) LP_{11} – LP_{01}, and (d) LP_{11}–LP_{11} modes. Note that the gray curve is the result of a Lorentzian fit for each.

The measured BGS for each of the pump–probe pairs are shown in Figs. 4(a)–4(d). A dominant gain peak is observed for the cases of LP_{01} – LP_{01}, LP_{01} – LP_{11}, and LP_{11} – LP_{01}, which are decently fitted with a Lorentzian curve (gray curve). In the case of LP_{11}–LP_{11}, two peaks with different amplitudes appeared, which can be fitted with two Lorentzian curves.

The ν_B and the width [full width at half-maximum (FWHM)] of the BGS for different pairs of the pump and the probe are listed in Table 2. It is notable that the ν_B of the intermodal SBS (LP_{01} – LP_{11} and LP_{11}–LP_{01}) is different from that of LP_{01}–LP_{01} by a small but nonnegligible amount (2 MHz) considering the accuracy of the measurement (<0.5 MHz). Meanwhile, larger differences (–25 MHz, 7 MHz) are observed between the ν_B's of the cases of LP_{11}–LP_{11} and LP_{01}–LP_{01}. Since the polarization dependence of ν_B estimated from the measured birefringence (3.5×10^{-5}) of the fiber is only about 0.3 MHz, the ν_B differences are mainly related to the acoustic velocity and the effective refractive indices based on the phase-matching condition for SBS, which is given by

$$\nu_B = V_a \cdot \left(\frac{n_1}{\lambda_1} + \frac{n_2}{\lambda_2}\right) \approx \frac{V_a}{\lambda} \cdot (n_1 + n_2), \qquad (1)$$

Table 1. MSC Ports for Different Pairs of the Pump and the Probe

Pump	Probe	Pump Input	Detection
LP_{01}	LP_{01}	TMF	TMF
LP_{01}	LP_{11}	TMF	SMF
LP_{11}	LP_{01}	SMF	TMF
LP_{11}	LP_{11}	SMF	SMF

Table 2. Characteristics of the BGS

Pump	Probe	ν_B (GHz)	FWHM (MHz)
LP_{01}	LP_{01}	10.641	29.6
LP_{01}	LP_{11}	10.639	32.8
LP_{11}	LP_{01}	10.639	32.5
LP_{11}	LP_{11}	10.616 (peak1)	27.1
		10.648 (peak2)	32.6

Table 3. Comparison Between the Experiment and the Simulation Results

Experiment			
Pump–probe	LP_{01}–LP_{11}	LP_{11}–LP_{11} (low)	LP_{11}–LP_{11} (high)
$\Delta\nu_B$ (LP_{01}–LP_{01}, MHz)	−2	−25	+7
Simulation			
Pump–probe	LP_{01}–LP_{11} (by L_{11})	LP_{11}–LP_{11} (by L_{01})	LP_{11}–LP_{11} (by L_{02})
$\Delta\nu_B$ (LP_{01}–LP_{01}, MHz)	−1	−28	+9

where λ_1 (λ_2) and n_1 (n_2) are the wavelength and the effective refractive index of the pump (probe) wave, and V_a is the phase velocity of the acoustic wave.

The interference pattern of the pump and the probe is symmetric in the cases of LP_{01}–LP_{01} and LP_{11}–LP_{11} and antisymmetric in the cases of LP_{01}–LP_{11} and LP_{11}–LP_{01}, considering the transverse distribution of the electric field. Therefore, one could attribute the SBS of LP_{01}–LP_{01} and LP_{11}–LP_{11} to symmetric acoustic modes, such as the L_{01} mode, and the intermodal SBS to antisymmetric acoustic modes, such as the L_{11} mode [10]. For theoretical confirmation, we carried out numerical simulations to calculate the velocity of leaky acoustic modes in the FUT assuming the elliptic core as a circular core with the same area [10]. The results were applied to Eq. (1) for the evaluation of ν_B with the effective indices of 1.4494 and 1.4456 for LP_{01} and LP_{11} modes, respectively, which were measured by prism output coupling [11]. The simulation results are compared to the experiments in Table 3. One can see that the shift of the ν_B ($\Delta\nu_B$) for each mode pair from that of LP_{01}–LP_{01} decently matches with the theoretical values calculated from different acoustic modes. It is also remarkable that two peaks appearing in the case of LP_{11}–LP_{11} can be explained by L_{01} and L_{02} modes, respectively, and the latter even provides larger Brillouin gain in Fig. 4(d).

In order to compare the relative amplitudes of the Brillouin gain for a pulse, a 50 ns (FWHM) Gaussian pulse at a repetition rate of 900 kHz was used as a probe (inset "B" in Fig. 2), and the amplitude was measured as a function of pump power (continuous wave). The frequency offset of the pump and the probe was set to the ν_B for each pair of modes. The results are depicted in Figs. 5(a)–5(d), which match well with a line fit with a slope of 0.053, 0.031, and 0.025 dB/mW for the cases of LP_{01}–LP_{01}, LP_{01}–LP_{11} (or LP_{11}–LP_{01}), and LP_{11}–LP_{11} (for larger peak), respectively. It is noticeable that the gain of the intermodal SBS is as large as about 58% of that of the SBS between the LP_{01} modes. The case of LP_{11}–LP_{11} shows a bit smaller Brillouin gain (~47% of the case of LP_{01}–LP_{01}) in Fig. 5(d), possibly due to the smaller overlap between the acoustic and electric fields.

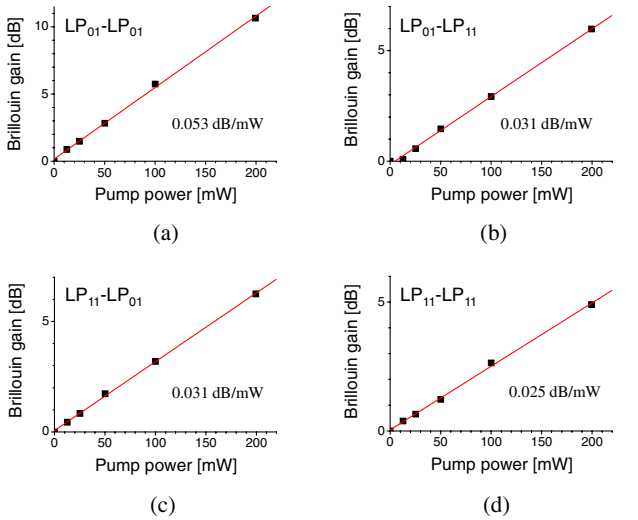

Fig. 5. Brillouin gain as a function of pump power for the pump–probe pairs of (a) LP_{01}–LP_{01}, (b) LP_{01}–LP_{11}, (c) LP_{11}–LP_{01}, and (d) LP_{11}–LP_{11}, plotted with a line fit for each.

In conclusion, the characterization of the SBS in an *e*-core TMF was demonstrated for different pairs of the optical modes using an MSC. We think the intermodal SBS could be observed in circular-core two- or few-mode fibers as well, and expect this phenomenon to become a new platform providing unique functions for the applications of two- or few-mode fibers.

This work was supported by a National Research foundation of Korea (NRF) grant funded by the Korean Ministry of Education, Science, and Technology (MEST) (2012-009103).

References

1. A. Al Amin, A. Li, X. Chen, and W. Shieh, Electron. Lett. **47**, 606 (2011).
2. N. Hanzawa, K. Saitoh, T. Sakamoto, T. Matsui, S. Tomita, and M. Koshiba, in *Optical Fiber Communication Conference*, OSA Technical Digest (CD) (Optical Society of America, 2011), paper OWA4.
3. S. Randel, R. Ryf, A. Sierra, P. J. Winzer, A. H. Gnauck, C. A. Bolle, R. J. Essiambre, D. W. Peckham, A. McCurdy, and R. Lingle, Jr., Opt. Express **19**, 16697 (2011).
4. B. Y. Kim, J. N. Blake, S. Y. Huang, and H. J. Shaw, Opt. Lett. **12**, 729 (1987).
5. P. St. J. Russell, D. Culverhouse, and F. Farahi, Electron. Lett. **26**, 1195 (1990).
6. B. Ward and M. Mermelstein, Opt. Express **18**, 1952 (2010).
7. W. V. Sorin, B. Y. Kim, and H. J. Shaw, Opt. Lett. **11**, 581 (1986).
8. K. Y. Song, I. K. Hwang, S. H. Yun, and B. Y. Kim, IEEE Photon. Technol. Lett. **14**, 501 (2002).
9. H. S. Park, K. Y. Song, S. H. Yun, and B. Y. Kim, J. Lightwave Technol. **20**, 1864 (2002).
10. C. K. Jen, A. Safaai-Jazi, and G. W. Farnell, IEEE Trans. Ultrason. Ferroelectr. Freq. Control **33**, 634 (1986).
11. W. V. Sorin, B. Y. Kim, and H. J. Shaw, Opt. Lett. **11**, 106 (1986).